Polymer Bulletin (2021) 78:2663–2684
https://doi.org/10.1007/s00289-020-03233-0

ORIGINAL PAPER

Comparative study of catalase immobilization via adsorption on P(MMA-co-PEG500MA) structures as an effective polymer support

Evren Sel[1] · Ahmet Ulu[1] · Burhan Ateş[1] · Süleyman Köytepe[1]

Received: 27 December 2019 / Revised: 28 March 2020 / Accepted: 16 May 2020 /
Published online: 24 May 2020

Abstract

In this study, poly[methyl methacrylate-co-poly(ethylene glycol) methacrylate] (P(MMA-co-PEG500MA)) copolymers were used for catalase (CAT) immobilization. Firstly, P(MMA-co-PEG500MA) copolymers were synthesized by using different amount of methyl methacrylate (MMA) and poly(ethylene glycol) methacrylate (PEG500MA) monomers. The synthesized copolymers were characterized by different analysis techniques. Afterward, CAT enzyme was immobilized via physical adsorption method onto the P(MMA-co-PEG500MA) copolymers. P3 sample containing 1:1 (PEG500MA:MMA) monomer molar ratio was selected as model support because of exhibiting optimum surface porosity and thermal stability. A high immobilization yield (76%) was achieved under optimized conditions. The immobilized enzyme displayed improved tolerance towards pH and temperature changes. After immobilization, the optimum pH shifted from 7.5 to 7.0, whereas the optimum temperature remained unchanged at 35 °C. Immobilized enzyme showed good reuse potential and excellent storage stability. After 10 consecutive uses, immobilized enzyme maintained about 51.0% of its initial activity. Furthermore, free enzyme completely lost its initial activity after 4 weeks, while immobilized enzyme maintained approximately 65% of the initial activity at 25 °C. Approximately twofold decrease in Km was obtained which means that the affinity of enzyme to the substrate improved after immobilization. Finally, it can be concluded that the prepared P(MMA-co-PEG500MA) copolymer structure can be an ideal matrix for CAT immobilization.

Keywords Enzyme immobilization · Catalase · Copolymer · Reusability

✉ Süleyman Köytepe
suleyman.koytepe@inonu.edu.tr

[1] Department of Chemistry, Faculty of Science and Literature, Inonu University, 44280 Malatya, Turkey

Introduction

Polymeric materials are an important part of our daily life and have very important functional tasks [1–5]. In particular, the polymers to be used in the production of optical, electronic, energy storage, sensors, food packaging and biological implants must have a high structural strength [6–9]. Especially, the synthesis of polymeric structures which can be used in many biomedical, bio-stable, drug release system and enzyme immobilization applications is seen as an important target in today's technology [8–10]. However, many applications during the adaptation of polymeric structures to technology require the synthesis of more robust, durable and bio-stable structures [9, 10]. In particular, in the field of biomaterials, flexible, durable, biocompatible, low toxicity and non-allergenic polymer structures are important [8–10].

All these researches have led to the formation of a new generation of materials with synthetic polymers and biocompatible surfaces. Particularly biocompatible polymers or oligomers grafted onto synthetic polymers are important for high technological applications [11–13]. Such structures are widely used in optical and electronic materials, especially in sensor and biosensor applications, energy storage applications, sample purification and sample enrichment applications, antibacterial surfaces, polymer supported catalysts, cell culture, enzyme immobilization matrix and tissue engineering [11, 13–17]. Especially, the use of biosuitable functional polymers, graft copolymers and polymer brushes is becoming widespread in enzyme immobilization applications [18–20]. Polymer brushes and graft copolymers having a large number of functional groups, soft, flexible, high surface area, have emerged as suitable candidates for immobilization of enzymes [18]. In this field, enzymes such as catalase, glucose oxidase and trypsin are immobilized to polymers structures by covalent or physical adsorption [18–21].

CAT (hydrogen peroxide oxidoreductase; EC.1.11.1.6), an oxidoreductase, is an important enzyme consisting of four subunits, each of which contains porphyrin heme (iron) as a prosthetic group [22]. It is widely distributed in animals, plants and all aerobic microorganisms, and it catalyzes the conversion of H_2O_2 to molecular oxygen and water [23]. However, as with most enzymes, CAT exhibits a short shelf life, low operational stability and reusability, which limits its potential application [24]. To overcome these limitations, enzyme immobilization is one of the important strategies. It is well known that the immobilized enzyme has many advantages such as improved stability, easy separation and recovery in comparison with free enzyme [25]. Till now, CAT was immobilized to many different carriers such as natural polymers [26], composites [27], nanoparticles [24], nanotubes [22], nanospheres [28] and metal organic framework (MOF) [29]. For instance, CAT was immobilized onto the PVA/PA6–Cu(II) nanofibrous membrane prepared via the electrospinning technique. The amount of immobilized CAT was reported as 64 ± 4.6 mg/g [30]. In another study, Inanan used p(2-hydroxyethyl methacrylate-chitosan)-Cu nanostructures as support for CAT immobilization and maximum amount of immobilized CAT was detected as 11.29 g/g support [28]. Rafiee-Pour et al. reported that CAT was immobilized onto the surfaces of

magnetic multiwalled carbon nanotubes via physical adsorption with ~ 60% yield [22]. Immobilized CAT has a wide range of uses in diverse industry such as biotechnology, biochemical analysis, sensor applications, food packaging, wastewater, pharmaceuticals and textiles [22, 28, 31]. In addition, to ensure long-term stability, usage of polymeric matrix is important in CAT immobilization [32–34]. PMMA as the immobilization matrix is generally used for different enzymes in many studies [35–37]. The preparation of copolymers or composites to enhance the enzyme immobilization properties of PMMA is commonly used techniques [38–40]. In this study, PMMA copolymer structures with high polarity monomer such as PEGMA were prepared and used in CAT immobilization. We showed here that P(MMA-co-PEG500MA) copolymers were easy to prepare and can be used as carrier matrix for CAT immobilization without notable losses in catalytic activity. The copolymers were characterized by various techniques such as elemental analysis, FTIR, TGA, DSC, SEM and EDX. Subsequently, the CAT enzyme was immobilized on different P(MMA-co-PEG500MA) copolymers via adsorption. To the best of our knowledge, this work is the first report using of P(MMA-co-PEG500MA) copolymers as support to immobilize CAT. The P(MMA-co-PEG500MA) copolymers synthesis and CAT immobilization processes are illustrated in Fig. 1. In terms of tolerance towards pH and temperature, reusability, storage stability and kinetic study, the properties of immobilized CAT were investigated and compared to the free enzyme. The outcomes reveal that the synthesized P(MMA-co-PEG500MA) copolymers may be a promising alternative carrier matrix for the immobilization and industrial applications of CAT.

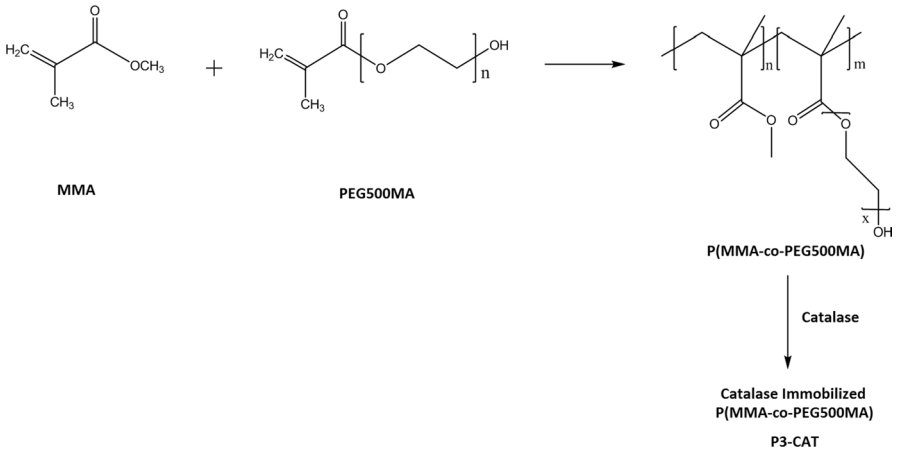

Fig. 1 Synthesis of P(MMA-co-PEG500MA) copolymers and immobilization of CAT

Materials and methods

Materials

Homopolymers (PMMA, PPEG500MA) and copolymers (P1, P2, P3, P4 and P5) were prepared with different amount MMA and PEG500MA monomers. PEG500MA structure with an average molecular mass of 500 was preferred. In the synthesis of copolymers, MMA structure was used as comonomer. Seven different polymeric structures were obtained by using different feed molar ratios of the monomers. These feed molar ratios of the MMA and PEG500MA as monomers are given in Table 1. The copolymers and homopolymers were distinguished by the various feed molar ratios of the monomers, e.g., sample 50/50 indicates the copolymer for the synthesis of which 50% PMMA and 50% PEG500MA were employed as the molar feed composition. The basic monomers, initiators used in the synthesis of copolymers and CAT from bovine liver (lyophilized powder, 2.000–5.000 units/mg protein) were obtained from Sigma-Aldrich. H_2O_2, toluene, xylene, tetrahydrofuran (THF) and *N*,*N*-dimethylformamide (DMF) were purchased Merck. All other chemicals were of analytical grade. All aqueous solutions were prepared by using ultrapure water.

Equipment

The copolymer structures synthesized as enzyme immobilization matrix were characterized in detail by elemental analysis and FTIR techniques. LECO-96CNOS device was used in elemental analyses. PerkinElmer Spectrum Two model FTIR spectrophotometer was used for FTIR analysis. Structural analyses were performed with ATR equipment in the wavelength range of 400–4000 cm^{-1}. Besides, copolymeric structures synthesized were examined by thermal analysis techniques in terms of glass transition temperatures, thermal decomposition temperatures and thermal stability. Thermal decomposition steps were measured on Shimadzu TGA-50 device, and thermal decomposition structures of homo and copolymers were determined. The glass transition temperatures (T_g) were measured on the Shimadzu DSC-60 instrument. α-Al_2O_3 was used as reference material in these analyses. Within a heating rate of 10°/min, the samples were thermally treated to 300 °C and 700 °C

Table 1 The molar ratios of the monomers in synthesis of PPEG500MA, PMMA and P(MMA-co-PEG500MA) structures

	MMA (%)	PEG500MA (%)
PPEG500MA	0	100
P1	20	80
P2	40	60
P3	50	50
P4	60	40
P5	80	20
PMMA	100	0

for DSC and TGA analysis, respectively. In addition, the UV spectrophotometer (Shimadzu, 1601) was used to measure the activity of free and immobilized enzyme.

Synthesis of poly(ethyleneglycol) side chain copolymer structures

Polyethylene glycol side chain copolymers were synthesized by free radical polymerization technique. Azobisisobutyronitrile (AIBN) was used as the initiator in this synthesis, and the monomers were prepared by dissolving with xylene solvent. The following procedure was used as the synthesis method. For synthesis of P3, PEG500MA (5 mmol) was added into a two-neck flask equipped with a magnetic stirrer and was dissolved in 5 mL xylene. 5 mmol of MMA monomer and 0.01 g of AIBN were added in PEG500MA solution in nitrogen atmosphere. The mixture was refluxed at 90 °C for 3 h. The resulting polymeric structure was then precipitated by adding 20 mL of methanol and washed with water and methanol. Seven polymeric structures were prepared by using same procedure with different molar ratios of the monomers (MMA/PEG500MA monomer ratios (mmol): 10/0; 8/2; 6/4; 5/5; 4/6; 2/8 and 0/10) (Table 1). It was synthesized in homopolymer structures using uniform monomer in copolymer synthesis according to the procedure. The completion of the reaction was checked by FTIR spectroscopy technique.

Enzyme immobilization

Hundred milligrams of copolymeric sample was placed in an Eppendorf tube. One milliliter of CAT enzyme solution (4 mg/mL) was added into the tube. The mixture was incubated for 12 h at 200 rpm on a shaker. The copolymer sample was then centrifuged at 5000 rpm for 5 min at 4 °C. The supernatant was stored to calculate the immobilization efficiency. The sample was washed thoroughly with PBS buffer to remove unbound CAT enzyme and dried at room temperature. Immobilized enzyme was stored at 4 °C to examine immobilization parameters such as optimum pH, optimum temperature, and storage stability.

Determination of total protein and immobilization efficiency (IE)

Total protein amount was determined according to the Bradford method using bovine serum albumin (BSA) as standard [41]. Immobilization efficiency was calculated using the following formula.

$$\mathrm{IE} = \left[\frac{(A_0 - B_1 - B_2)}{A_0}\right] \times 100$$

A_0 is the total protein amount of the free enzyme, and B_1 and B_2 are the amount of protein of the supernatant and washing solution after immobilization.

Enzyme activity of free and immobilized enzyme

Free enzyme activity was determined spectrophotometrically by measuring the decrease in H_2O_2 absorbance at 240 nm in a reaction mixture containing 1.0 mL of substrate (pH: 7.5, 20 mM H_2O_2) and 20 µL of CAT (2 mg/mL). The reaction mixture was maintained at 25 °C for 2 min, and the enzymatic reaction was stopped by adding 0.5 mL of 1 M HCl. For immobilized enzyme activity, copolymeric samples (5 mg) were mixed with the substrate solution prepared as above at 25 °C for 2 min. After 2 min, the samples were removed and then the reaction was stopped by adding 0.5 mL of 1 M HCl. One unit (U) of enzyme activity was defined as the quantity of enzyme catalyzing the decomposition of 1 µmol H_2O_2 per min under optimum assay conditions [31]. The maximum activity in all enzyme results was assumed to be 100%, and the results were given as relative activity. In addition, all enzyme activity measurements were carried out using three parallel samples and standard deviations were added to the corresponding graphs.

Effect of pH and temperature

The effect of pH on free and immobilized enzyme activity was investigated by using 0.5 M sodium acetate buffer (pH 4.0, 5.0, 6.0), 0.5 M sodium phosphate buffer (pH 7.0, 7.5, 8.0) and 0.5 M Tris–HCl buffer (pH 8.5–9.0) at different pH values. Additionally, the effect of temperature on free and immobilized enzyme activity was measured in a controlled temperature water bath from 25 to 60 °C under standard assay conditions.

Reusability

Reusability of the immobilized enzyme was also investigated. The immobilized enzyme was exposure to fresh H_2O_2 solution, and the activity was measured according to assay activity. After washing the immobilized enzyme, it was exposed to the same concentration of substrate again. This procedure was repeated 20 times, and the enzyme activity was measured after each step. The activity of the enzyme after the first use was considered 100%.

Determination of kinetic parameters

The Michaelis constant (Km) and maximum reaction velocity (V_{max}) of free and immobilized enzyme were determined by varying the substrate concentration in the range of 2–20 mM in phosphate buffer (pH 7.5, 10 mM) at room temperature (~ 25 °C). Km and V_{max} values were calculated from enzyme activities corresponding to different concentrations using Lineweaver–Burk plot of $1/S$ versus $1/V$ [42].

$$1/V = (\mathrm{Km}/V_{max})\,(1/S) + 1/V_{max}$$

where V is rate of reaction, [S] is the concentration of substrate, Km is Michaelis–Menten constant and V_{max} is maximum reaction rate.

Storage stability

Free and immobilized enzyme samples were stored at 4 °C and room temperature (~25 °C), and their activity was measured periodically during 4 weeks. The initial activities of both samples were considered 100%.

Results and discussion

Characterization of P(MMA-co-PEG500MA) structures

Firstly, elemental analysis data were evaluated for the characterization of PMMA, PPEG500MA and copolymer structures and the results are shown in Table 2 in together with theoretical values. According to these results, even in different copolymer structures, elemental analysis results were found to be very close to theoretical values.

The FTIR spectra of prepared homopolymer and copolymer structures are shown in Fig. 2. Firstly, in the FTIR spectra of pure PMMA, a sharp stretching peak

Table 2 Elemental analysis results of synthesized PPEG500MA, PMMA and P(MMA-co-PEG500MA) structures

Sample	C	H
PPEG500MA		
Calculated	54.80	8.72
Found	53.30	7.96
P1		
Calculated	55.05	8.69
Found	54.74	9.24
P2		
Calculated	55.41	8.64
Found	54.60	8.01
P3		
Calculated	55.67	8.60
Found	56.34	8.09
P4		
Calculated	56.01	8.56
Found	57.05	7.52
P5		
Calculated	57.12	8.40
Found	57.01	7.33
PMMA		
Calculated	60.03	8.00
Found	55.75	8.11

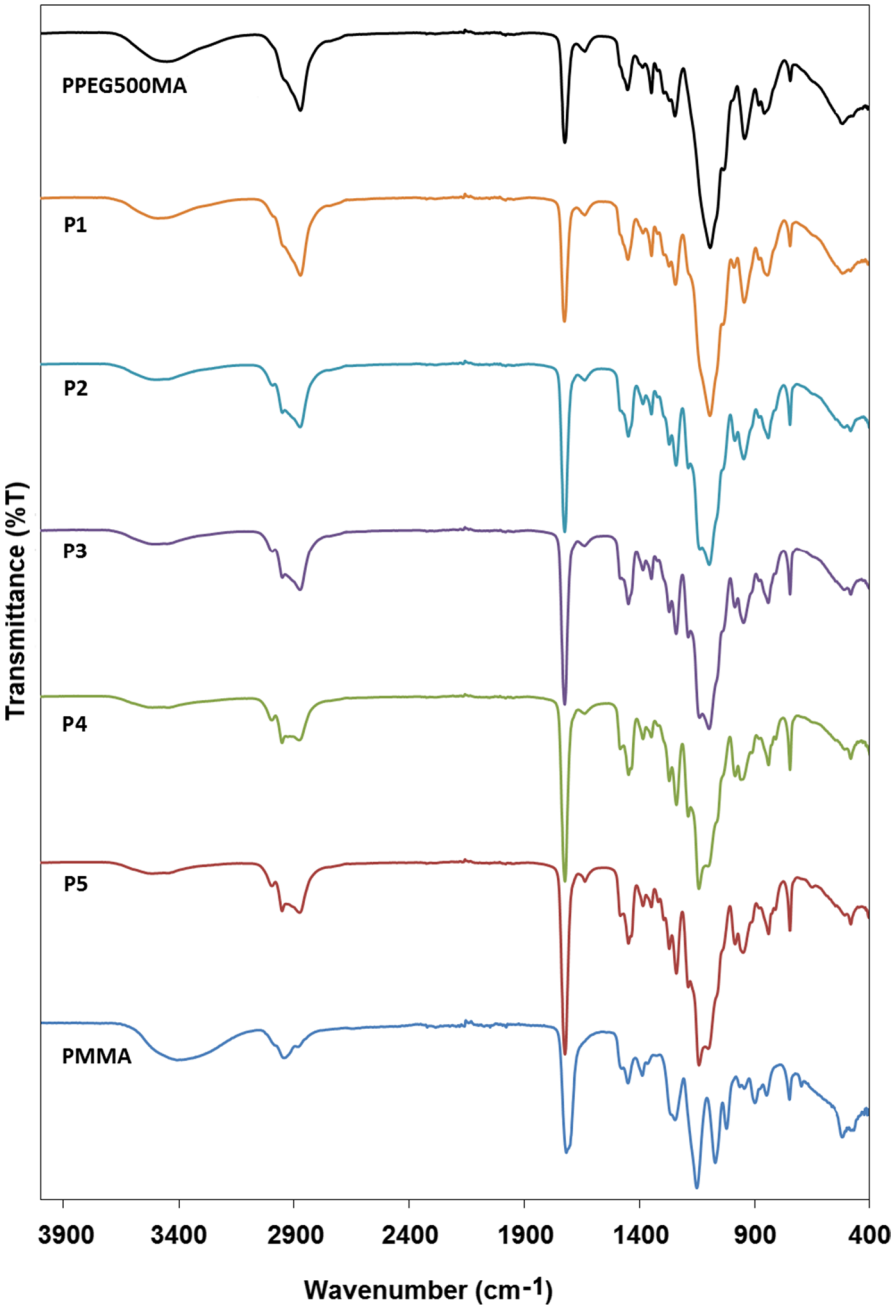

Fig. 2 FTIR spectra of PPEG500MA, PMMA and P(MMA-co-PEG500MA) copolymer structures

stem from the carboxyl group was found at 1735 cm^{-1}. Aliphatic C–H stretching vibration at 2899–2950 cm^{-1} was observed. The peaks at 1274 cm^{-1} are assigned to the stretching vibration of the ester bond C–O. The other important peaks at 1195 cm^{-1} and 1144 cm^{-1} are assigned to the stretching of –O–CH_3 unit and the CH_3 group, respectively. According to FTIR spectrum results, the broad –OH band at 3300–3600 cm^{-1} was observed in the spectra of PPEG500MA, PMMA and P(MMA-co-PEG500MA) copolymer structures. However, as expected, –OH band expanded obviously with the increase in the PEG500MA ratio in the copolymer structure. The aliphatic C–H stretching was observed at 2830 cm^{-1} and 2970 cm^{-1} in all copolymer FTIR spectra. Another important peak is the carbonyl group stretching peak due to the ester structure of methacrylate unit in copolymer structures. This carbonyl peak appeared at 1820 cm^{-1}. In addition, the C–H bending peak of the aliphatic CH_2 products and C–C stretching were observed at 1430 cm^{-1} and 1380 cm^{-1}, respectively. C–O–C etheric stretching peak at 1190 cm^{-1} and CH_2 rocking vibration at 751 cm^{-1} also appeared [43, 44]. These FTIR spectra show that the polymerization process has been successfully carried out.

Thermal analysis of P(MMA-co-PEG500MA) structures

The thermal properties of PPEG500MA, PMMA and P(MMA-co-PEG500MA) structures were investigated by TGA, DTG and DSC analysis. Figure 3 shows the TGA thermogram of PPEG500MA, PMMA and P(MMA-co-PEG500MA) structures. This figure shows two different types of thermograms. The polymers containing the PEG500MA structure exhibit similar thermograms, while the thermogram of the PMMA structure is different from the others. This is because PMMA has a rigid polymer structure which is frequently stacked, while other structures have the characteristic of oligo-ethylene glycol side groups. In the TGA thermogram of PMMA, a

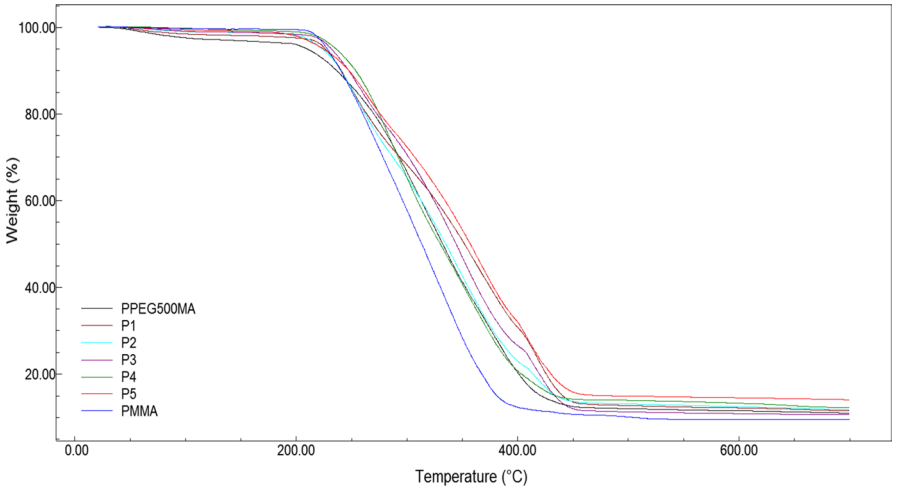

Fig. 3 TGA thermograms of PPEG500MA, PMMA and P(MMA-co-PEG500MA) structures

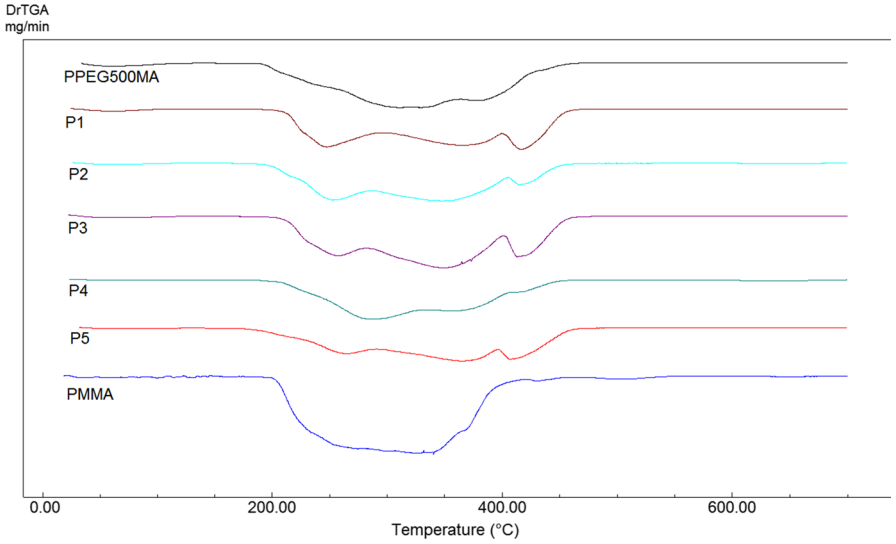

Fig. 4 DTGA thermograms of PPEG500MA, PMMA and P(MMA-co-PEG500MA) structures

clear weight loss was observed about between 220 and 400 °C [45]. This weight loss associated with random scission and thermal degradation of the polymer backbone. Thermograms of the copolymer structures were seen in similar. These thermograms show two weight losses. The initial weight loss values of the copolymers are due to the moisture that depends on the structure. The second weight loss is due to the degradation of the polymeric structure. The derivative thermogravimetric analysis

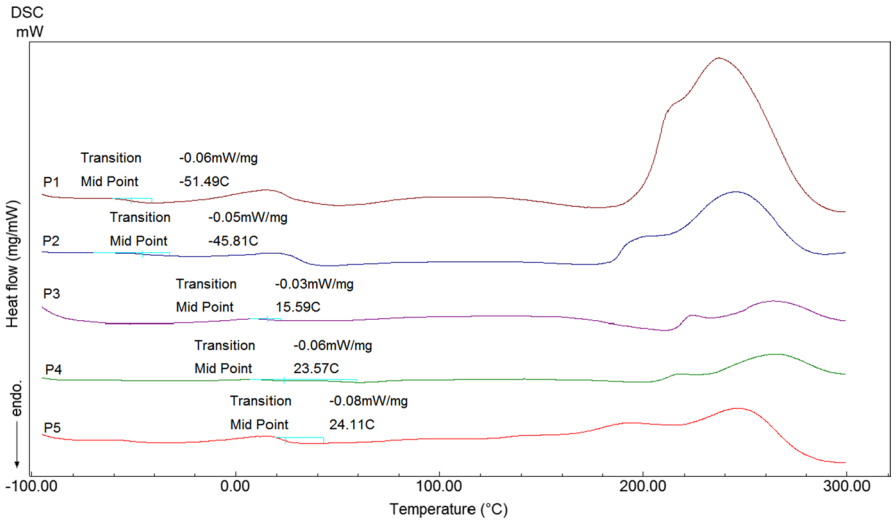

Fig. 5 DSC thermograms of P(MMA-co-PEG500MA) structures

(DTGA) curves of PPEG500MA, PMMA and P(MMA-co-PEG500MA) structures in the temperature range from 0 to 700 °C are compared in Fig. 4. The DTGA curve of pure PMMA showed show single-stage degradation peak. This peak is thermal degradation of the polymer between 200 and 400 °C. There are also three degradation peaks in the DTGA curves of the copolymer structures [46, 47]. The first peak stems from degradation of side groups. The other peaks are due to the thermal degradation of polymeric structure [47]. DTGA curves of P(MMA-co-PEG500MA) structures are compatible with the TGA thermogram of copolymeric structures.

In Fig. 5, DSC thermograms and T_g values of copolymers were given. When these values were examined, it was seen that the T_g value of the copolymer decreases depending on the ratio of PEG500MA in the copolymer structure. Especially, in DSC thermograms of P1 and P2 structures, a peak stem from the removal of moisture in the structure can be seen between 40 and 110 °C. Because the ratio of PEG500MA in the copolymer structure is high in these structures, hydrophilicity is high. This reduction is due to the opening of the interchain distance by the introduction of the oligo-ethylene glycol structure between the polymer chains. In the PEG500MA subgroup, this increases the flexibility of the polymer in biomedical applications and facilitates its applicability.

Surface morphologies of PPEG500MA, PMMA and P(MMA-co-PEG500MA) structures

The SEM images of pure PPEG500MA (a), P(MMA-co-PEG500MA) (b) and pure PMMA (c) structures are presented in Fig. 6. Especially in pure PMMA and pure PPEG500MA structures, the surface looks more homogeneous and smoother. However, with the conversion of the polymer structure to the copolymer structure, the porosity of the structure and its applicability in terms of biomedical applications increase. In Fig. 7, SEM images of copolymer structures were detailed by giving different magnification rates. In these images, the surface morphology of the copolymer structures was given in two different magnification ratios. As the PEG500MA ratio increases, the roughness of the surface increased in 5000 × and 2500 × SEM images. The low- and high-magnification SEM images in Fig. 6 provide information on the surface roughness and porosity of the polymers to be used for enzyme immobilization. Homopolymers, P1, P4 and P5 have a very flat and non-fractal morphology. Therefore, these structures are not preferred for enzyme immobilization. Although P2 and P3 structures have a fractal surface, P3 structure has a more porous and rough surface than P2. Therefore, the P3 structure was preferred for enzyme immobilization. Detailed SEM images of P3 structure are given in Fig. 7 at different magnifications. The P3 structure has large cavities and porosity, especially at low magnifications.

In the SEM and thermal analyzes carried out within the scope of the study, it was determined that P3 structure containing 1:1 (PEG500MA:MMA) monomer molar ratio was the most suitable structure for enzyme immobilization. Particularly in SEM analysis, suitable porosity was observed in P3 (PEG500MA content 50%). This is due to the fact that there are free voids on the acrylate polymer to which

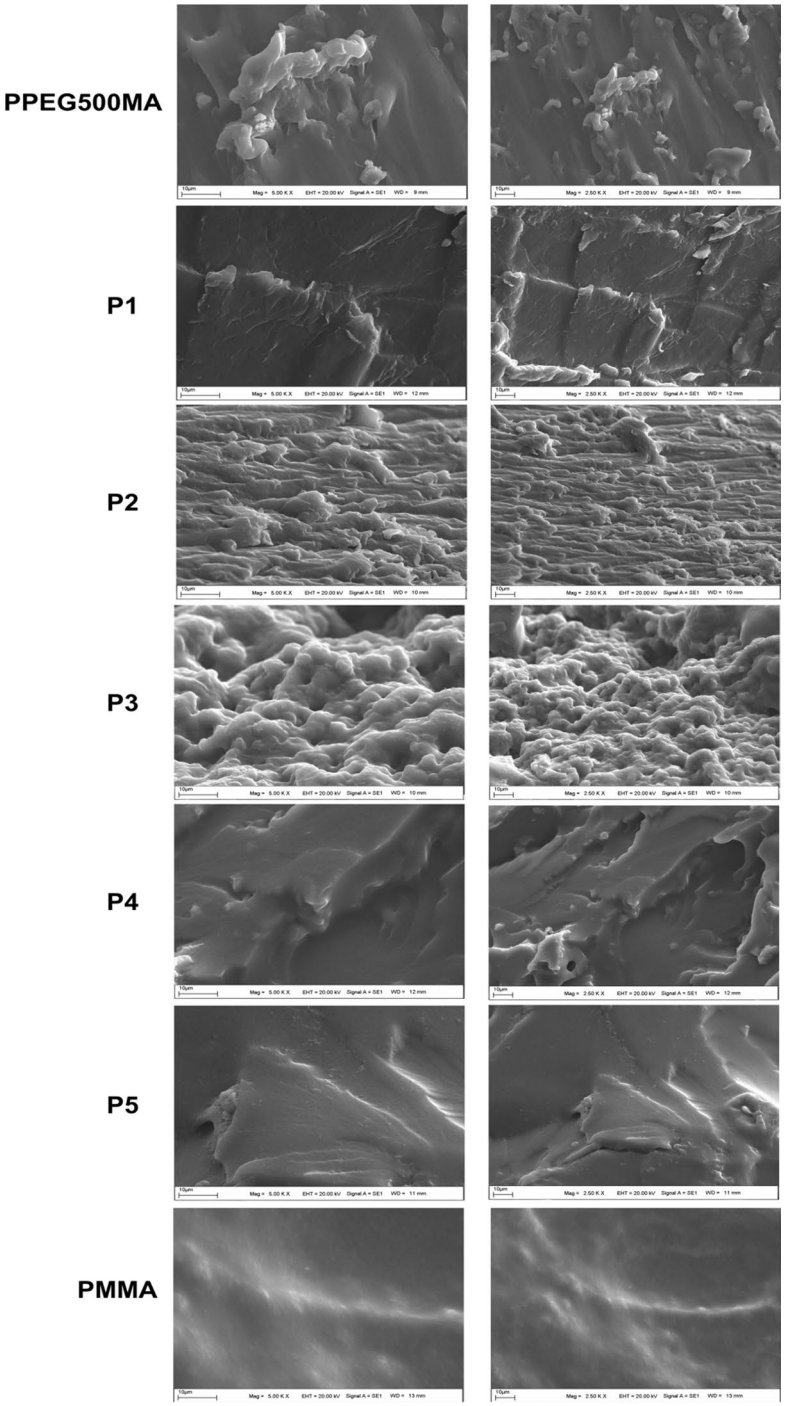

Fig. 6 SEM images of pure PPEG500MA, P(MMA-co-PEG500MA) copolymer structures and pure PMMA

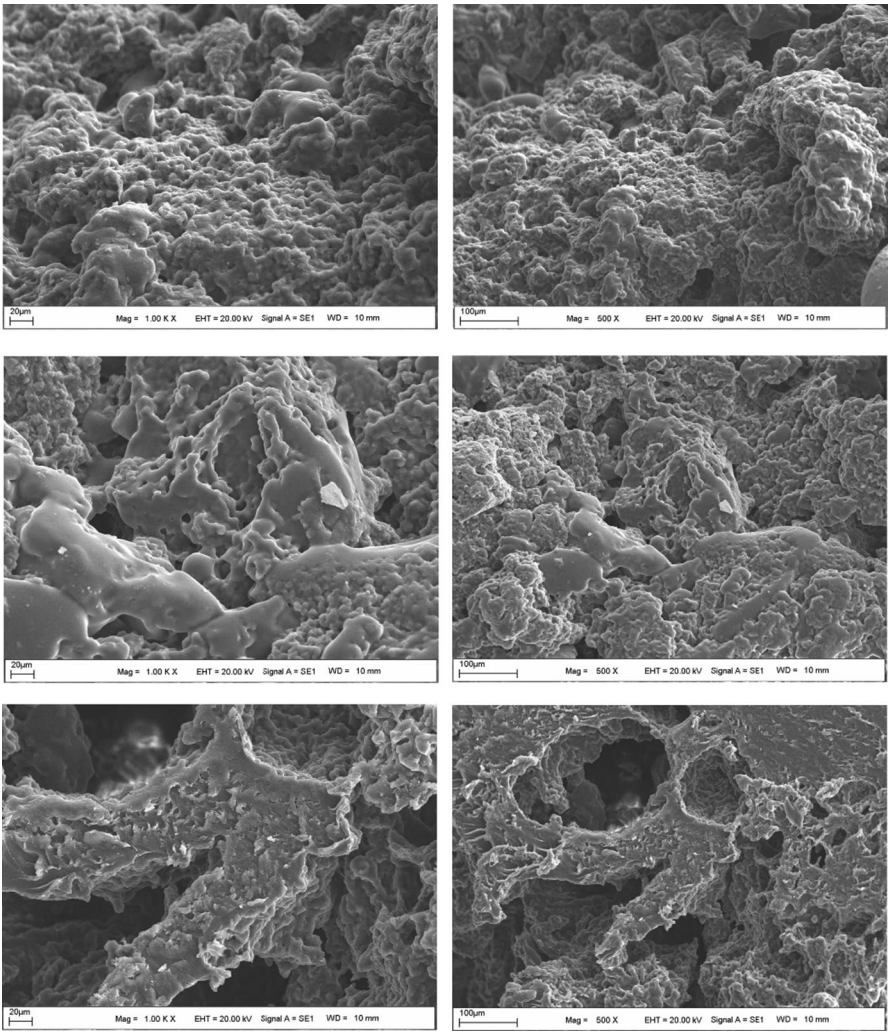

Fig. 7 Detailed SEM images of P3 structures

the oligo-ethylene glycol structure is attached, which is compatible with the SEM structure. For this reason, enzyme immobilization studies were carried out with this optimally selected structure.

Binding confirmation

In addition, the presence of CAT on surface of P3 was confirmed via FTIR, SEM and EDX analysis. The FTIR spectra for pure P3 and P3-CAT are shown in Fig. 8. A broad absorption band at 3000–3600 cm^{-1} (–OH stretching vibrations and –NH stretching vibrations) indicated the presence of enzyme on the copolymer [48].

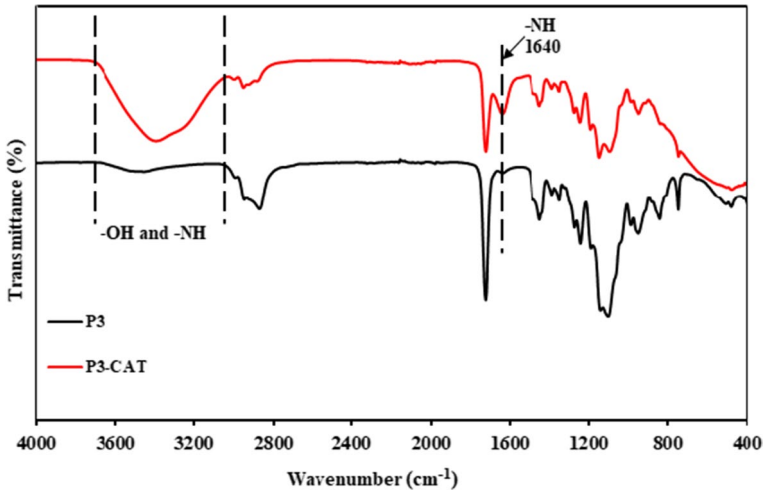

Fig. 8 FTIR spectra of P3 and P3-CAT

Besides, the signal at 1640 cm^{-1} observed on the P3-CAT was due to NH bending of CAT [49], although no such signal was observed for pure P3. The FTIR analysis results were ensured the success of immobilization.

To further investigate the presence of CAT on the P3 structure, the SEM analysis was performed. As presented in Fig. 9, compact pores were observed on the surface of P3, whereas a rough and non-uniform coating was observed on the surface of the P3-CAT. The morphological changes on the surface indicated that the CAT enzyme was successfully immobilized onto the P3.

In addition, the immobilization of enzyme on the support was also observed with EDX (Fig. 10). The P3 included only carbon (C) and oxygen (O) elements, whereas nitrogen (N) and sulfur (S) peaks appeared in the EDX pattern of P3-CAT. It is obvious that the presence of N and S peaks was due to the amino acid residues of CAT. Besides, elemental mapping results indicated successfulness of CAT immobilization on support and collaborated with FTIR and EDX analysis.

Immobilization efficiency

The enzyme immobilization efficiency for the P3 copolymer was calculated using the formula mentioned in "Determination of total protein and immobilization efficiency (IE)" section. The immobilization efficiency was 76%. This high yield can be attributed to the interactions between the copolymer and the enzyme.

Effect of pH and temperature

The effect of pH on the activity of the free and immobilized enzyme was investigated in the pH range 4.0–10.0. As seen from Fig. 11, the enzymatic activities of

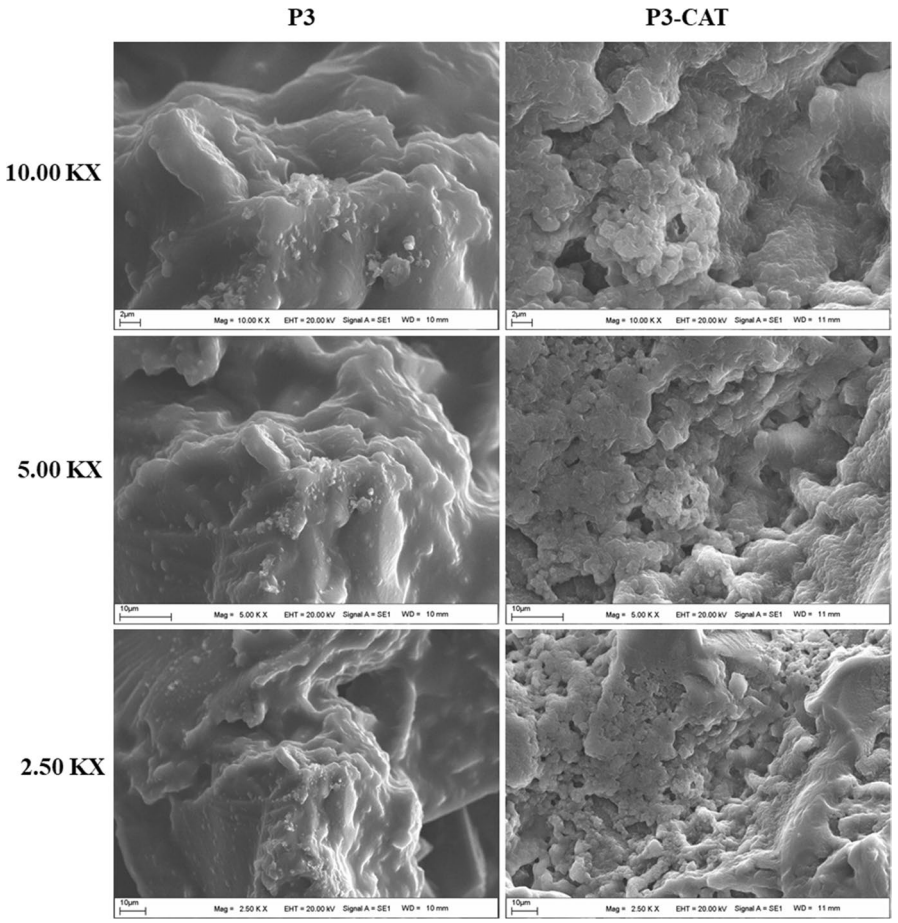

Fig. 9 The SEM images of P3 and P3-CAT at different magnifications

free and immobilized enzyme were optimal at pH values of 7.5 and 7.0, respectively. A shift of 0.5 units in pH optimum may be due to conformational changes after immobilization. Under acidic conditions (pH 4–6), free enzyme possessed more activity, while the immobilized enzyme maintained higher enzymatic activity in pH range of 8.0–10.0 compared to free one. The free enzyme retained only 16% of its original activity, whereas the relative activity of immobilized enzyme had more than 56% at pH 10 thanks to suitable support.

The effect of temperature on free and immobilized enzyme was investigated, as shown in Fig. 12. Both free and immobilized enzyme exhibited maximum activity at 35 °C. As the temperature was increased, the activities of both free and immobilized enzyme reduced; however, the immobilized enzyme displayed greater activity than that of free one at each temperature value. For instance, the free enzyme retained 28% of its original activity, whereas the relative activity

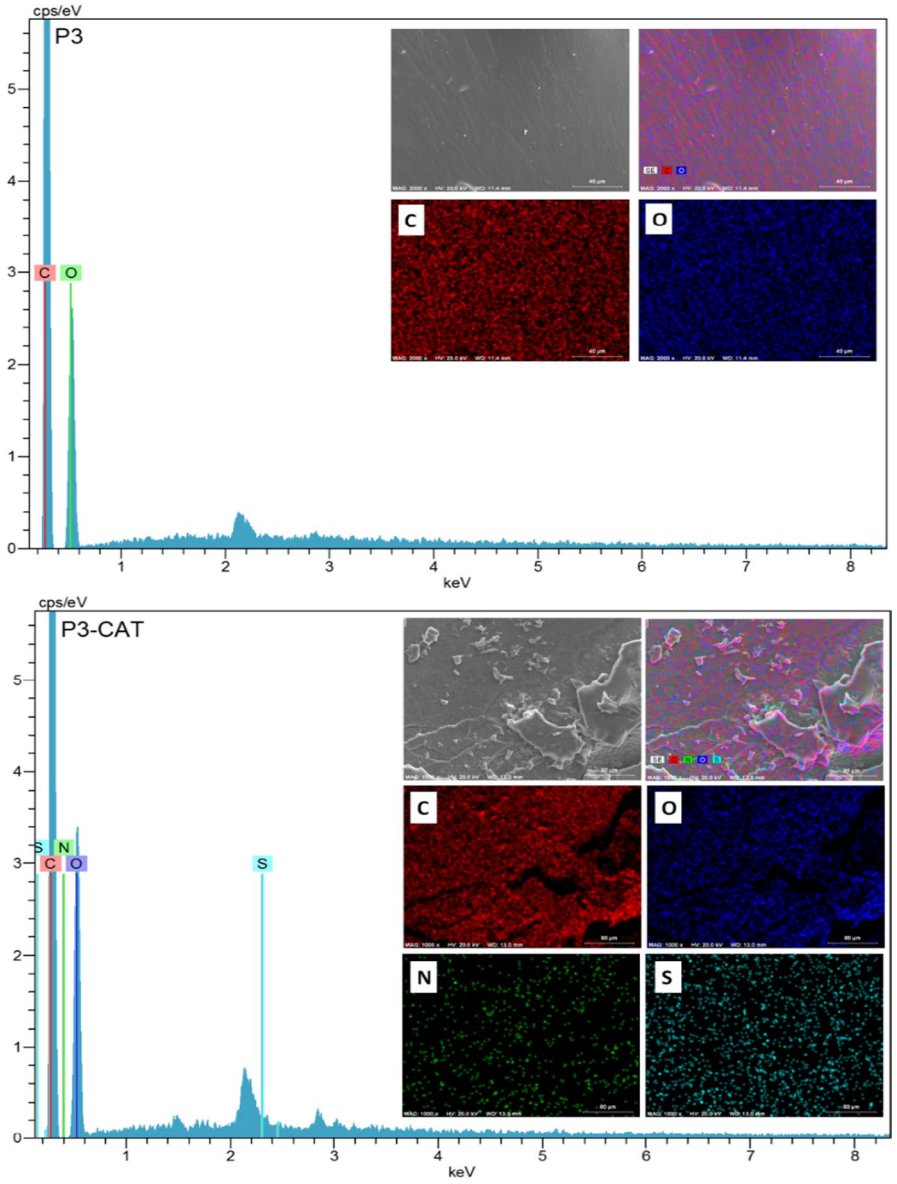

Fig. 10 The EDX spectra and elemental mapping images of P3 and P3-CAT

of immobilized enzyme had about 40% at 65 °C. These results suggested that the free enzyme exposed to conformational changes as the temperature increases, resulting in a rapid decrease in activity. In contrast, the immobilized enzyme has a more stable conformation due to interactions between the support and the enzyme. Therefore, it exhibited improving activity under harsh conditions [50, 51].

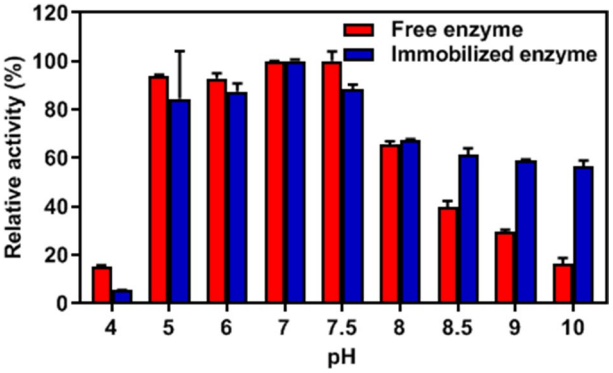

Fig. 11 Effect of pH on the activity of free and immobilized enzyme

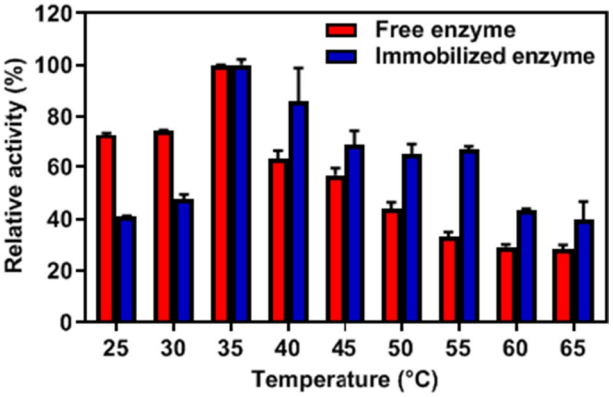

Fig. 12 Effect of temperature on the activity of free and immobilized enzyme

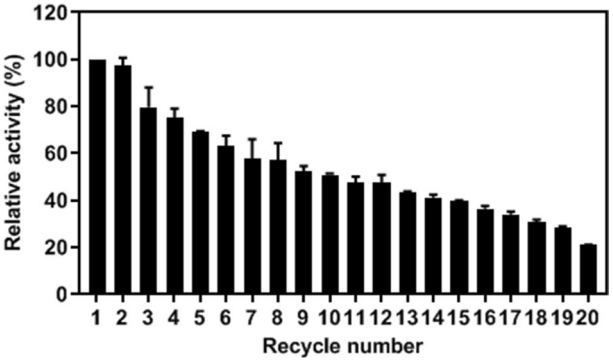

Fig. 13 Repeatability test of immobilized enzyme

Reusability and storage stability

The reusability of the immobilized enzymes is an important parameter for their application in industry. To determine the reusability of the immobilized enzyme, the activity of it was repeated 20 times. As shown in Fig. 13, the immobilized enzyme maintained more than 70% of its original activity after the initial five uses and remained above 51% for another five measurements. After 20 cycle repeated uses, the immobilized enzyme retained about 21% of its original activity. The reduction in activity could attribute to deactivation or leakage of enzyme during repeated use. Consequently, the high reusability results indicated that immobilized enzyme is more stable and advantageous in comparison with free counterpart.

The storage stability results for the free and immobilized enzyme at 4 °C and 25 °C are shown in Fig. 14. According to these results, immobilized enzyme maintained its initial activity more than free enzyme at both 4 °C and 25 °C. The immobilized enzyme retained nearly 90% of its initial activity after 4 weeks, whereas the activity of free enzyme protected 72% for under the same conditions (Fig. 14a). At 25 °C, the free enzyme completely lost its initial activity after 4 weeks, while

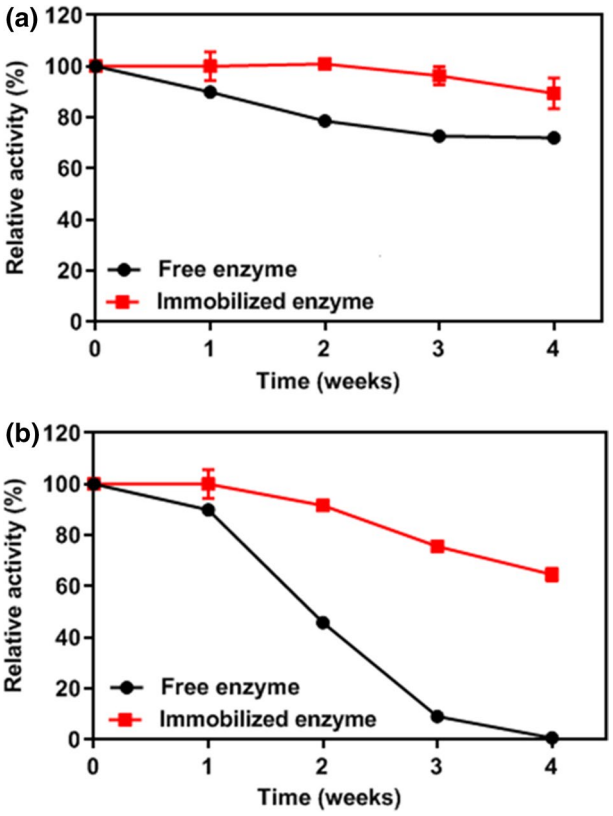

Fig. 14 Storage stability results for free and immobilized enzyme (**a** 4 °C and **b** 25 °C)

Table 3 Kinetic parameters for free and immobilized enzyme

	Km (mM)	V_{max} (μmol H_2O_2/mg min)
Free enzyme	102	909
Immobilized enzyme	49	1666

the immobilized enzyme maintained approximately 65% of the initial activity (Fig. 14b). It is clear that that the P(MMA-co-PEG500MA) is a good and promising support for CAT immobilization with excellent long-term stability.

Kinetic parameters

The Km and V_{max} for free and immobilized enzyme are calculated and summarized in Table 3. Km and V_{max} values for free enzyme were estimated as 102 mM and 909 μmol H_2O_2/mg min, respectively. After immobilization, Km and V_{max} values changed 49 mM and 1666 μmol H_2O_2/mg min, respectively. The small Km value indicates that the enzyme has a high catalytic efficiency at a low substrate concentration [51]. The Km value for immobilized enzyme decreased about 2.0-fold. This significant change in the Km value can be attributed to the high accessibility of the substrate molecules to the active sites of immobilized enzyme. Similar results were also reported by other studies. For instance, Inanan reported that the Km value decreased 2.4-fold when compared with the free one [28]. Çetinus et al. revealed that the immobilized enzyme on chitosan beads exhibited a decrease of approximately 2.0 times in Km value [52]. Similarly, Erol et al. reported that Km value decreased approximately 2.0 times after immobilization on poly(HEMA-GMA) cryogels [53]. In addition, the V_{max} value for immobilized enzyme was about 1.8-fold higher than that of the free counterpart. Generally, the enhancements in V_{max} resulted from substrate diffusion ratio, conformation changes or cooperative effects of enzymes [54, 55].

Conclusions

The oligo-ethylene glycol side groups on the polymer chain, with a mechanical barrier and strong hydrogen bonding properties, prevent the enzyme from leaking from the polymer structure and form a suitable immobilization medium. As proof of this, P(MMA-co-PEG500MA) copolymer structures were successfully synthesized via free radical polymerization technique and used as an ideal support for enzyme immobilization. CAT which is an important industrial enzyme was used as a model enzyme and was successfully immobilized onto copolymer structures. Compared with the free enzyme, the immobilized enzyme displayed improved pH and temperature tolerance under harsh conditions. Additionally, it exhibited excellent reusability and long-term stability in comparison with free one. Therefore, the synthesized P(MMA-co-PEG500MA) structures can be a facile and efficient support for

CAT immobilization. In view of the above information, more copolymer structures should be synthesized in the near future to find more promising carrier material candidate for the immobilization of different enzymes, and applications.

Compliance with ethical standards

Conflict of interest There are no conflicts of interest to declare.

References

1. Koushal V, Sharma R, Sharma M, Sharma R, Sharma V (2014) Plastics: issues challenges and remediation. Int J Waste Resour 4(1):134
2. Raheem D (2012) Application of plastics and paper as food packaging materials—an overview. Emir J Food Agric 25(3):177–188
3. Mülhaupt R (2013) Green polymer chemistry and bio-based plastics: dreams and reality. Macromol Chem Phys 214:159–174
4. Ignatyev IA, Thielemans W, Vander Beke B (2014) Recycling of polymers: a review. ChemSusChem 7:1579–1593
5. Luzi F, Torre L, Kenny JM, Puglia D (2019) Bio- and fossil-based polymeric blends and nanocomposites for packaging: structure–property relationship. Materials (Basel) 12(3):471
6. Othman SH (2014) Bio-nanocomposite materials for food packaging applications: types of biopolymer and nano-sized filler. Agric Agric Sci Procedia 2:296–303
7. Fan B, Zhou M, Zhang C, He D, Bai J (2019) Polymer-based materials for achieving high energy density film capacitors. Prog Polym Sci 97:101143
8. Balakrishnan P, Geethamma VG, Sreekala MS, Thomas S (2018) Polymeric biomaterials: state-of-the-art and new challenges. In: Thomas S, Balakrishnan P, Sreekala MS (eds) Woodhead publishing series in biomaterials, fundamental biomaterials: polymers. Woodhead Publishing, Sawston, pp 1–20
9. Shah SA, Sohail M, Khan S, Minhas MU, de Matas M, Sikstone V, Hussain Z, Abbasi M, Kousar M (2019) Biopolymer-based biomaterials for accelerated diabetic wound healing: a critical review. Int J Biol Macromol 139:975–993
10. Abbasian M, Massoumi B, Mohammad-Rezaei R, Samadian H, Jaymand M (2019) Scaffolding polymeric biomaterials: are naturally occurring biological macromolecules more appropriate for tissue engineering? Int J Biol Macromol 134:673–694
11. Feng C, Huang X (2018) Polymer brushes: efficient synthesis and applications. Acc Chem Res 51(9):2314–2323
12. Advincula RC, Brittain WJ, Caster KC, Ruehe J (2004) Polymer brushes. Wiley-VCH, Weinheim
13. Milner ST (1991) Polymer brushes. Science 251:905–914
14. Zhao B, Brittain WJ (2000) Polymer brushes: surface-immobilized macromolecules. Prog Polym Sci 25:677–710
15. Bumbu GG, Kircher G, Wolkenhauer M, Berger R, Gutmann JS (2004) Synthesis and characterization of polymer brushes on micromechanical cantilevers. Macromol Chem Phys 205:1713–1720
16. Krishnamoorthy M, Hakobyan S, Ramstedt M, Gautrot JE (2014) Surface-initiated polymer brushes in the biomedical field: applications in membrane science, biosensing, cell culture, regenerative medicine and antibacterial coatings. Chem Rev 114:10976–11026
17. Koenig M, König U, Eichhorn K-J, Müller M, Stamm M, Uhlmann P (2019) In-situ-investigation of enzyme immobilization on polymer brushes. Front Chem 7(101):1–8
18. Koenig M, Bittrich E, König U, Rajeev BL, Müller M, Eichhorn K-J, Thomas S, Stamm M, Uhlmann P (2016) Adsorption of enzymes to stimuli-responsive polymer brushes: influence of brush conformation on adsorbed amount and biocatalytic activity. Colloids Surf B Biointerfaces 146:737–745

19. del Castillo GF-D, Koenig M, Müller M, Eichhorn K-J, Stamm M, Uhlmann P, Dahlin A (2019) Enzyme immobilization in polyelectrolyte brushes: high loading and enhanced activity compared to monolayers. Langmuir 35:3479–3489
20. Xu FJ, Cai QJ, Li YL, Kang ET, Neoh KG (2005) Covalent immobilization of glucose oxidase on well-defined poly(glycidyl methacrylate)−Si(111) hybrids from surface-initiated atom-transfer radical polymerization. Biomacromolecules 6(2):1012–1020
21. Qin W, Song Z, Fan C, Zhang W, Cai Y, Zhang Y, Qian X (2012) Trypsin immobilization on hairy polymer chains hybrid magnetic nanoparticles for ultra fast, highly efficient proteome digestion, facile 18O labeling and absolute protein quantification. Anal Chem 847:3138–3144
22. Rafiee-Pour HA, Nejadhosseinian M, Firouzi M, Masoum S (2019) Catalase immobilization onto magnetic multi-walled carbon nanotubes: optimization of crucial parameters using response surface methodology. New J Chem 43:593–600
23. Arabaci G, Usluoglu A (2013) Catalytic properties and immobilization studies of catalase from *Malva sylvestris* L. J Chem 686185:1–6
24. Czechowska E, Ranoszek-Soliwoda K, Tomaszewska E, Pudlarz A, Celichowski G, Gralak-Zwolenik D, Szemraj J, Grobelny J (2018) Comparison of the antioxidant activity of catalase immobilized on gold nanoparticles via specific and non-specific adsorption. Colloids Surf B Biointerfaces 171:707–714
25. Zhang L, Sun Y (2018) Poly(carboxybetaine methacrylate)-grafted silica nanoparticle: a novel carrier for enzyme immobilization. Biochem Eng J 132:122–129
26. Costa SA, Reis RL (2004) Immobilisation of catalase on the surface of biodegradable starch-based polymers as a way to change its surface characteristics. J Mater Sci Mater Med 15(4):335–342
27. Kaushal J, Seema SG, Arya SK (2018) Immobilization of catalase onto chitosan and chitosan–bentonite complex: a comparative study. Biotechnol Rep 18(e00258):1–6
28. Inanan T (2019) Chitosan co-polymeric nanostructures for catalase immobilization. React Funct Polym 135:94–102
29. Feng Y, Zhong L, Bilal M, Tan Z, Hou Y, Jia S, Cui J (2018) Enzymes@ZIF-8 nanocomposites with protection nanocoating: stability and acid-resistant evaluation. Polymers (Basel) 11:1–14
30. Feng Q, Zhao Y, Wei A, Li C, Wei Q, Fong H (2014) Immobilization of catalase on electrospun PVA/PA6–Cu(II) nanofibrous membrane for the development of efficient and reusable enzyme membrane reactor. Environ Sci Technol 48(17):10390–10397
31. Bayramoglu G, Karagoz B, Yilmaz M, Bicak N, Arica MY (2011) Immobilization of catalase via adsorption on poly(styrene-d-glycidylmethacrylate) grafted and tetraethyldiethylenetriamine ligand attached microbeads. Bioresour Technol 102(4):3653–3661
32. Murtinho D, Lagoa AR, Garcia FAP, Gil MH (1998) Cellulose derivatives membranes as supports for immobilisation of enzymes. Cellulose 5:299–308
33. Airoldi C, Monteiro Junior O (2003) Copper adsorption and enzyme immobilization on organosilane-glutaraldehyde hybrids as support. Polym Bull 50:61–68
34. Ingenbosch KN, Rousek A, Wunschik DS, Hoffmann-Jacobsen K (2019) A fluorescence-based activity assay for immobilized lipases in non-native media. Anal Biochem 569:22–27
35. Cerqueira MRF, Santos MSF, Matos RC, Gutz IGR, Angnes L (2015) Use of poly(methyl methacrylate)/polyethyleneimine flow microreactors for enzyme immobilization. Microchem J 118:231–237
36. Li S, Hu J, Liu B (2004) Use of chemically modified PMMA microspheres for enzyme immobilization. Biosystems 77(1–3):25–32
37. Bulmuş V, Ayhan H, Pişkin E (1997) Modified PMMA monosize microbeads for glucose oxidase immobilization. Chem Eng J Biochem Eng J 65(1):71–76
38. Lai Y, Wang F, Zhang Y, Ou P, Wu P, Fang Q, Li S, Chen Z (2019) Effective removal of methylene blue and orange II by subsequent immobilized laccase decolorization on crosslinked polymethacrylate/carbon nanotubes. Mater Res Express 6(085541):1–11
39. Pugazhenthi G, Kumar A (2004) Enzyme membrane reactor for hydrolysis of olive oil using lipase immobilized on modified PMMA composite membrane. J Membr Sci 228:187–197
40. Ulu A, Koytepe S, Ates B (2016) Synthesis and characterization of PMMA composites activated with starch for immobilization of L-asparaginase. J Appl Polym Sci 43421:1–11
41. Bradford MM (1976) A rapid and sensitive method for the quantitation of microgram quantities of protein utilizing the principle of protein-dye binding. Anal Biochem 72:248–254
42. Patil PD, Yadav GD (2018) Rapid in situ encapsulation of laccase into metal-organic framework support (ZIF-8) under biocompatible conditions. ChemistrySelect 3:4669–4675

43. Kanimozhi G, Vinoth S, Harish K, Srinadhu E, Satyanarayana N (2019) Conductivity and dielectric permittivity studies of KI-based nanocomposite (PEO/PMMA/KI/I2/ZnO nanorods) polymer solid electrolytes. Polym Compos 40:2919–2928
44. Abdelrazek E, Elashmawi I, Soliman M, Aly A (2009) Physical properties of $MnCl_2$ fillers incorporated into a PVDF/PVC blend and their complexes. J Vinyl Addit Technol 15:171–177
45. Poomalai P, Varghese TO, Siddaramaiah (2011) Thermomechanical behaviour of poly(methylmethacrylate)/copoly(ether-ester) blends. Int Sch Res Netw ISRN Mater Sci 2011:1–5
46. Ramírez-Jiménez A, Montoya-Villegas KA, Licea-Claverie A, Gónzalez-Ayón MA (2019) Tunable thermo-responsive copolymers from DEGMA and OEGMA synthesized by RAFT polymerization and the effect of the concentration and saline phosphate buffer on its phase transition. Polymers 11:1657
47. Tsai B, Garcia-Valdez O, Champagne P, Cunningham MF (2017) Poly(poly(ethylene glycol) methyl ether methacrylate) grafted chitosan for dye removal from water. Processes 5(12):1–13
48. Asmat S, Husain Q, Azam A (2017) Lipase immobilization on facile synthesized polyaniline-coated silver-functionalized graphene oxide nanocomposites as novel biocatalysts: stability and activity insights. RSC Adv 7:5019–5029
49. Saleem M, Rafiq M, Seo SY, Lee KH (2016) Acetylcholinesterase immobilization and characterization, and comparison of the activity of the porous silicon-immobilized enzyme with its free counterpart. Biosci Rep 36(art:00311):1–11
50. Patel SKS, Otari SV, Chan Kang Y, Lee JK (2017) Protein-inorganic hybrid system for efficient his-tagged enzymes immobilization and its application in l-xylulose production. RSC Adv 7:3488–3494
51. Samui A, Sahu SK (2018) One-pot synthesis of microporous nanoscale metal organic frameworks conjugated with laccase as a promising biocatalyst. New J Chem 42:4192–4200
52. Çetinus ŞA, Öztop HN, Saraydin D (2007) Immobilization of catalase onto chitosan and cibacron blue F3GA attached chitosan beads. Enzyme Microb Technol 41(4):447–454
53. Erol K, Cebeci BK, Köse K, Köse DA (2019) Effect of immobilization on the activity of catalase carried by poly(HEMA-GMA) cryogels. Int J Biol Macromol 123:738–743
54. Kumar A, Patel SKS, Mardan B, Pagolu R, Lestari R, Jeong SH, Kim T, Haw JR, Kim SY, Kim IW, Lee JK (2018) Immobilization of xylanase using a protein-inorganic hybrid system. J Microbiol Biotechnol 28(4):638–644
55. Sharma N (2013) Kinetic study of free and immobilized protease from Aspergillus sp. IOSR J Pharm Biol Sci 7(2):86–96